

## Surface pole figures by reflection high-energy electron diffraction

F. Tang,<sup>a)</sup> G.-C. Wang, and T.-M. Lu

Department of Physics, Applied Physics and Astronomy, Rensselaer Polytechnic Institute, 110 8th Street, Troy, New York 12180-3590

(Received 17 June 2006; accepted 30 October 2006; published online 11 December 2006)

The authors demonstrated that it is possible to construct a reflection high-energy electron diffraction (RHEED) pole figure of a polycrystalline film by recording multiple RHEED patterns as they rotate the substrate around the surface normal. Since electrons have limited penetration depth, the pole figure constructed is a surface pole figure. It is in contrast with the conventional x-ray pole figure which gives an average texture information of the entire film. Surface texture change, particularly the evolution of multiple preferred orientations, in polycrystalline Ru films grown by oblique angle vapor deposition has been observed using this RHEED surface pole figure technique. © 2006 American Institute of Physics. [DOI: 10.1063/1.2403916]

The preferred crystalline orientation, or texture, is a fundamental property of polycrystalline film and it directly controls many important physical properties such as optical, magnetic, mechanical, and electrical properties of the films. Texture formation is a very complex phenomenon. To date, the fundamental understanding of the atomistic mechanisms on the texture evolution still remains as a challenging subject.<sup>1</sup> Many effects such as surface diffusion, step barriers, sticking coefficient, surface energy, strain energy, and shadowing effect<sup>1-6</sup> can all play roles in the formation of a texture. To construct a realistic atomistic model, one requires a detailed knowledge on how the surface texture evolves at different stages of growth. This information is very often not available mainly due to the lack of experimental techniques that allow one to measure the surface texture quantitatively. The conventional x-ray pole figure gives an average texture of the entire thickness of the film since x-ray penetrates into the entire film.<sup>7</sup> As the texture of a film very often changes during growth, information on the surface texture evolution during growth is mostly lost in the x-ray pole figure analysis. In this letter we report the use of a conventional reflection high-energy electron diffraction (RHEED) technique to construct a surface pole figure, which can reveal the surface texture of polycrystalline films. The technique allows one to extract information on the dynamics of surface texture evolution.

RHEED has been a powerful technique for monitoring the epitaxy film growth.<sup>8,9</sup> Recent studies showed that RHEED can also be used to obtain information such as crystal phase, orientation, and grain size and shape from the diffraction patterns of polycrystalline films.<sup>10-14</sup> In this case, the electrons penetrate through small crystallites at the surface and a transmission electron diffraction pattern is formed. However, this RHEED pattern only gives partial information of the crystal orientation. A complete texture including the in-plane orientation may not be extracted from this pattern alone. In the present work, we construct a surface pole figure, to obtain a complete description of surface texture,<sup>7</sup> by recording multiple RHEED patterns as we rotate the substrate around the substrate normal. The use of a two-dimensional area detector to construct pole figures has been

reported in x-ray diffraction<sup>15-17</sup> and in transmission electron microscopy (TEM) operated in both transmission and reflection modes.<sup>18</sup> Compared with TEM, RHEED covers a larger surface area of the thin film and is suitable for *in situ* characterization of thin film growth.

In our RHEED experiments, the electron gun was operated at 9 kV and 0.25 mA emission current. The incident angle of electron beam on the sample is smaller than 1°. During the measurements, the vacuum pressure was less than  $7.0 \times 10^{-9}$  Torr. RHEED patterns imaged on a phosphor screen were acquired by using a charge-coupled device with a 16 bit dynamic range. Using an UHV step motor to rotate the substrate around the surface normal, the wobbling is minimized to less than 0.05°. The step motor has a step size of 1.8°. A total of 200 patterns covering azimuthal angle of 360° were recorded for the pole figure measurements. The exposure time for each image was 5 s. The total data collection time was ~20 min.

The samples used in this work were Ru films composed of either vertical or slanted nanorods. Figures 1(a) and 1(b) are scanning electron microscopy (SEM) cross sections of the vertical and slanted nanorods, respectively. These Ru films were grown by the oblique angle deposition using a dc magnetron sputtering system. The vertical nanorods were formed by substrate rotation while the slanted nanorods were formed with no substrate rotation during deposition. The details have been presented elsewhere.<sup>19</sup> The shadowing effect in the oblique angle deposition leads to these nanostructured films.<sup>20-22</sup>

To illustrate the process of constructing a surface pole figure through RHEED images, we use the film with vertical

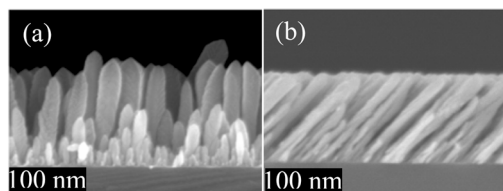


FIG. 1. (Color online) SEM cross-sectional view of (a) a Ru film with vertical nanorods (~340 nm thick) and (b) a Ru film with slanted nanorods (~440 nm thick). Under oblique angle sputter deposition the vertical nanorods were formed with substrate rotation while the slanted nanorods were formed with a fixed substrate. The scale bar is 100 nm.

<sup>a)</sup> Author to whom correspondence should be addressed; electronic mail: tangf2@rpi.edu

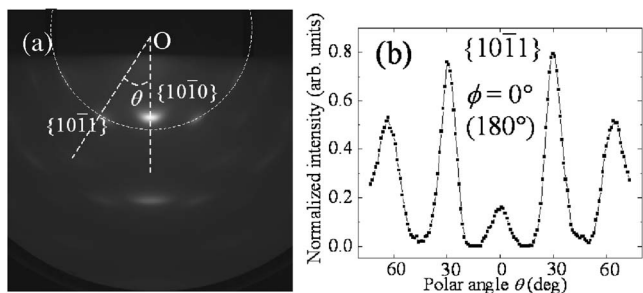


FIG. 2. (a) *Ex situ* RHEED pattern from the film with vertical Ru nanorods (~340 nm). The image consists of many concentric arcs. O is the origin point. The angle  $\theta$  is the polar angle measured along the diffraction arc from the substrate normal (vertical dashed line). (b) The normalized intensity of the  $\{10\bar{1}0\}$  ring [white dashed ring in (a)] is plotted as a function of the polar angle  $\theta$ . This intensity profile represents a slice from the  $\{10\bar{1}1\}$  pole figure at azimuthal angle  $\phi=0^\circ$  (or  $180^\circ$ ).

Ru nanorods (~340 nm thick) as an example. Figure 2(a) shows a typical RHEED pattern. The absence of a specular reflection spot indicates that this is a transmission pattern. The image is composed of many concentric arcs. For a particular family of crystal planes, for example, the  $\{10\bar{1}1\}$  labeled in Fig. 2(a), the related arcs are distributed in a circle (white dashed curve) having the same radius from the origin point O. The polar angle  $\theta$  is measured along the arc. It is the angle between the substrate normal and the direction connecting the origin and a point of interest on the arc. To construct the pole figure, we first plotted the normalized intensities of the  $\{10\bar{1}0\}$  as a function of the polar angle  $\theta$  along the circle in Fig. 2(b). (The detailed procedure of the intensity normalization is given in Ref. 23.) This intensity profile represents one “slice” of the  $\{10\bar{1}0\}$  pole figure at a particular azimuthal angle  $\phi$ , for example,  $\phi=0^\circ$  (or  $180^\circ$ ), shown in Fig. 2(b). Physically, the intensity of the plot corresponds to the distribution of orientation of crystalline grains. The width of the individual peak reflects the dispersion of the texture axis.<sup>10-14</sup>

The sample is then rotated around the surface normal to a different azimuthal angle  $\phi$  to take another diffraction pattern. Another slice of the pole figure is then obtained by measuring the intensity distribution along the ring with the same radius. The whole pole figure is then constructed by combining different slices at various azimuthal angles ranging from  $0^\circ$  to  $360^\circ$ . During the construction, the curvature of the Ewald sphere is also considered. However, its effects on the pole figure analysis are negligible.<sup>10,11</sup> The relationship between the pole figure and crystalline orientations can be illustrated in Fig. 3(a). In this figure the measured diffraction intensity of  $\{10\bar{1}1\}$  is distributed on a sphere. This intensity distribution corresponds to the orientation distribution of crystalline grains. The pole figure is actually a stereographic projection of the intensity distribution of the pole sphere onto a planar surface, which is illustrated in Fig. 3(a). Figure 3(b) shows the contour plot of the constructed  $\{10\bar{1}1\}$  pole figure from these intensity profiles. It illustrates the azimuthal symmetry of vertical Ru rods well. The solid black rings shown in Fig. 3(b) are calculated positions of the diffraction intensity of the  $\{10\bar{1}1\}$  pole figure assuming a perfect  $\{10\bar{1}0\}$  fiber texture. This fiber texture has one degree preferred orientation (I-O). The grains have no preferred ori-

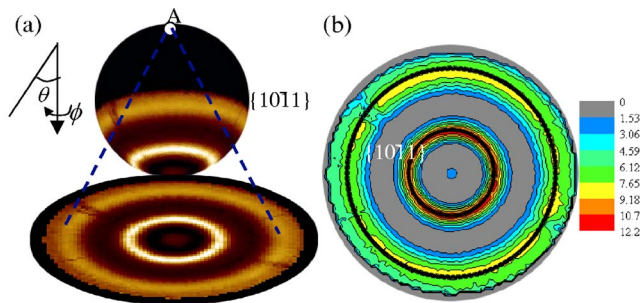


FIG. 3. (Color online) (a) Illustration of the stereographic projection of a pole sphere to obtain the pole figure of the film with vertical Ru nanorods. The angle  $\phi$  is the azimuthal angle. Point A is the polar of the pole sphere. The dashed lines indicate the projected directions. (b) The constructed  $\{10\bar{1}1\}$  pole figure is shown in a contour plot and displays a good azimuthal symmetry. The solid black rings are calculated intensity distributions of the  $\{10\bar{1}1\}$  pole figure assuming a perfect  $\{10\bar{1}0\}$  fiber texture. The increasing numbers indicates higher intensity in the bar graph.

entation in the plane of the substrate (in plane).

Unlike the film with vertical Ru nanorods, the film with slanted Ru nanorods exhibit much more complicated crystalline orientations. The  $\{10\bar{1}1\}$  and  $\{10\bar{1}0\}$  RHEED pole figures at deposition times of 5 and 60 min are shown in Figs. 4(a)–4(d). From these figures we can see that the pole figures do not have a ring structure but have discrete spots. This implies that in addition to the out-of-plane texture, the films possess in plane, or azimuthally, preferred orientation, known as the II-O structure<sup>6</sup> (labeled as  $\langle h_1k_1l_1 \rangle \langle h_2k_2l_2 \rangle$ ). The first notation represents the out-of-plane texture and the second notation shows the preferred azimuthal orientation. For a hexagonal-close-packed (hcp) structure, the notation of

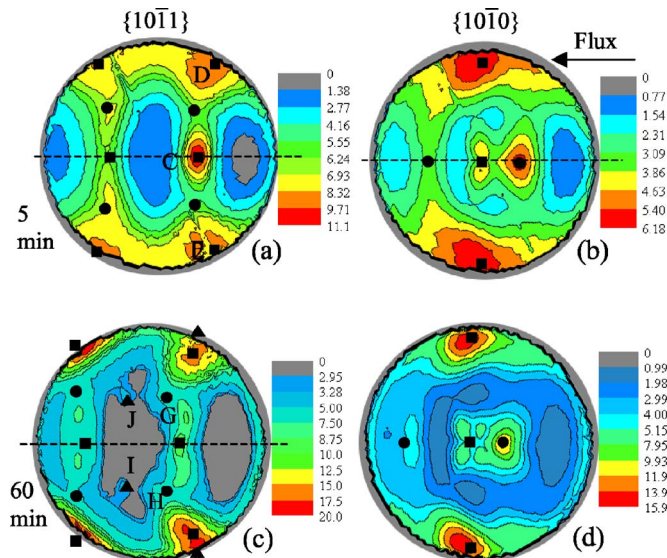


FIG. 4. (Color online) (a)  $\{10\bar{1}1\}$  (b)  $\{10\bar{1}0\}$  pole figures from a Ru film with slanted nanorods with 5 min deposition time (~33 nm thick). [(c) and (d)] Similar pole figures were constructed for a Ru film with slanted nanorods with 60 min deposition time (~440 nm thick). The  $\{10\bar{1}1\}\{10\bar{1}0\}$  and  $\{10\bar{1}0\}\{11\bar{2}0\}$  textures exist at both thicknesses. However, the  $\{10\bar{1}0\}\{11\bar{2}0\}$  becomes stronger and additional  $\{0001\}\{11\bar{2}0\}$  texture appears in the thicker film. The increasing numbers indicate a higher intensity in the bar graph. The C, D, E, I, J, G, and H are the center positions of the poles from the corresponding textures.

Miller indices for lattice planes is more convenient to represent the preferred orientation. A number of arguments, including shadowing and asymmetric surface diffusion, have been presented in the literature to explain the azimuthal angle selection.<sup>4-6,13</sup> But a general theory to accurately predict the orientation selection has not emerged.

The  $\{10\bar{1}1\}$  and  $\{10\bar{1}0\}$  RHEED pole figures have the symmetry with respect to the vapor incident plane indicated by the dashed lines shown in Figs. 4(a)–4(d). This vapor incident plane is also taken as the reference for determining the II-O textures, in which most crystallites point in two preferred directions within this plane. At 5 min deposition, several strong poles already emerging, as shown in Figs. 4(a) and 4(b), indicate that the II-O texture starts at an early stage of growth. We selected points C, D and E in the  $\{10\bar{1}1\}$  pole figure of Fig. 4(a), as examples to illustrate the texture orientation. The coordinate  $(\theta, \phi)$  of these points are  $(26^\circ, 0^\circ)$ ,  $(61^\circ, 62^\circ)$ , and  $(62^\circ, 297^\circ)$ . The angle between C and D ( $52.0^\circ$ ) and the angle between C and E ( $53.3^\circ$ ) are both close to the smallest angle ( $52.1^\circ$ ) between two  $\{10\bar{1}1\}$  family planes, for example,  $(10\bar{1}1)$  and  $(01\bar{1}1)$ . This suggests that C, D, and E have originated from the same II-O texture. The  $\{10\bar{1}1\}$  is one of the preferred crystalline directions in the vapor incident plane, which is tilted toward the flux at an angle  $\gamma=(26\pm 1)^\circ$  with respect to the substrate normal. Through similar analyses for Fig. 4(b) we also found the texture of  $\{10\bar{1}0\}\{11\bar{2}0\}$  ( $\gamma=(23\pm 1)^\circ$ ) at this thickness. Also shown in the figures are the calculated positions of the poles from ideal  $\{10\bar{1}1\}\{10\bar{1}0\}$  and  $\{10\bar{1}0\}\{11\bar{2}0\}$  textures. We can see that the calculated patterns match the experimental data very well.

The  $\{10\bar{1}1\}\{10\bar{1}0\}$  ( $\gamma=(21\pm 1)^\circ$ ) and  $\{10\bar{1}0\}\{11\bar{2}0\}$  ( $\gamma=(17\pm 1)^\circ$ ) textures with slightly different tilting angles also appear in the pole figures from 60 min deposited film [see Figs. 4(c) and 4(d)]. These features were also qualitatively observed in x-ray pole figures.<sup>19</sup> This is not surprising in that this thicker film is dominated by these two major orientations. However, the  $\{10\bar{1}0\}\{11\bar{2}0\}$  becomes stronger as indicated from the cusp shape structures around positions G and H. There are also two more distinct poles appearing around points J and I in the RHEED surface pole figures Fig. 4(c) which are not clearly resolved in the corresponding x-ray pole figures. The angle between these two poles is  $\sim 58^\circ$  and it suggests a weak  $\{0001\}\{11\bar{2}0\}$  ( $\gamma=(33\pm 1)^\circ$ ) texture.

We show that very rich surface texture information such as the II-O texture can be obtained from the RHEED pole figures from the films composed of slanted nanorods. Armed with this RHEED surface pole figure technique, one would be able to study how the texture changes during different stages of growth and also gain insights into factors that control the texture formation through atomistic models. The quality of data collection and RHEED pole figure construc-

tion can be further improved. For example, it would be desirable to put an energy filter in front of the phosphor screen to reduce the background intensity that comes from the inelastic scattering. In order to reduce the overlapping of adjacent diffraction rings, a medium energy electron beam can be used to increase the angular separation between rings.

This work has been supported in part by NSF NIRT (0506738). The authors thank T. Karabacak for providing the samples and T. Parker for taking SEM images of the samples.

<sup>1</sup>For review, see H. Huang, in *Handbook of Multiscale Materials Modeling*, edited by S. Yip (Springer Science and Business Media, New York, 2005), Sect. 2.30, p. 1039.

<sup>2</sup>C. V. Thompson, *Annu. Rev. Mater. Sci.* **30**, 159 (2000).

<sup>3</sup>Paritosh, D. J. Srolovitz, C. C. Battaile, X. Li, and J. E. Butler, *Acta Mater.* **47**, 2269 (1999).

<sup>4</sup>O. P. Karpenko, J. C. Bilello, and S. M. Yalisove, *J. Appl. Phys.* **82**, 1397 (1997).

<sup>5</sup>A. van der Drift, *Philips Res. Rep.* **22**, 267 (1967).

<sup>6</sup>E. Bauer, *Fiber Texture*, The Ninth National Vacuum Symposium of the American Vacuum Society, edited by George H. Bancroft (Macmillan, New York, 1963), p. 35.

<sup>7</sup>See, for example, B. D. Cullity, *Elements of X-ray Diffraction* (Addison-Wesley, Reading, MA, 1978), 2nd ed., p. 297.

<sup>8</sup>See, for example, A. Ichimiya and P. I. Cohen, *Reflection High Energy Electron Diffraction* (Cambridge, New York, 2005), Chap. 2, p. 4.

<sup>9</sup>J. I. Harris, B. A. Joyce, and P. J. Dobson, *Surf. Sci.* **103**, L90 (1981).

<sup>10</sup>Dmitri Litvinov, Thomas O'Donnell, and Roy Clarke, *J. Appl. Phys.* **85**, 2151 (1999).

<sup>11</sup>Stéphane Andrieu and Patrick Fréchard, *Surf. Sci.* **360**, 289 (1996).

<sup>12</sup>Jason T. Drotar, T.-M. Lu, and G.-C. Wang, *J. Appl. Phys.* **96**, 7071 (2004).

<sup>13</sup>F. Tang, C. Gaire, D.-X. Ye, T. Karabacak, T.-M. Lu, and G.-C. Wang, *Phys. Rev. B* **72**, 035432 (2005).

<sup>14</sup>F. Tang, T. Karabacak, P. Morrow, C. Gaire, G.-C. Wang, and T.-M. Lu, *Phys. Rev. B* **72**, 165402 (2005).

<sup>15</sup>K. Helming and U. Preckwinkel, *Solid State Phenom.* **105**, 71 (2005).

<sup>16</sup>S. L. Lee, D. Windover, M. Doxbeck, M. Nielsen, A. Kumar, and T.-M. Lu, *Thin Solid Films* **377**, 447 (2000).

<sup>17</sup>H. J. Bunge and H. Klein, *Z. Metallkd.* **87**, 465 (1996).

<sup>18</sup>B. Schäfer and R. A. Schwarzer, *Mater. Sci. Forum* **273–275**, 223 (1998).

<sup>19</sup>P. Morrow, F. Tang, T. Karabacak, P.-I. Wang, D.-X. Ye, G.-C. Wang, and T.-M. Lu, *J. Vac. Sci. Technol. A* **24**, 232 (2006).

<sup>20</sup>K. Robbie and M. J. Brett, *J. Vac. Sci. Technol. A* **15**, 1460 (1997).

<sup>21</sup>A. Lakhtakia and R. Messier, *Sculptured Thin Films: Nanoengineered Morphology and Optics* (SPIE, Bellingham, WA, 2005), Chap. 1, p. 7.

<sup>22</sup>T. Karabacak and T.-M. Lu, in *Handbook of Theoretical and Computational Nanotechnology*, edited by M. Rieth and W. Schommers (American Scientific, Stevenson Ranch, CA, 2005), Vol. 9, Chap. 69, p. 729.

<sup>23</sup>The procedure of intensity normalization is as follows. To obtain the intensity of a  $\theta$  value from the diffraction ring, which is used for constructing a pole figure, we first integrate the intensity across that ring at the polar angle. The diffraction patterns usually have a diffuse background due to the multiple and inelastic scatterings. Therefore, the integrated intensity is followed by a linear background subtraction. Next, the intensity, after background subtraction, is normalized by dividing the background intensity (Ref. 12). The value used for the background division normally is taken as the average of the linear background. But for the inner diffraction ring ( $\{10\bar{1}0\}$ ) the use of the background far from the shadowing edge gives an angular relationship without distortions between crystalline planes in the pole figures.